BES Analysis Memo

March 11, 1997

revised April 1, 1997

Study of $\psi_{2S} \to \gamma\ +\ 4$ charged tracks

Stephen L. Olsen

University of Hawaii

Abstract

We present results of a study the processes $\psi_{2S} \to \gamma +$ four charged tracks in the BES collaboration's sample of 3.5M ψ_{2S} decay events. We report measurements of branching fractions for $\eta_c(1S)$ and $\chi_{c0,1,2}$ decays to $2(\pi^+\pi^-)$, $\pi^+\pi^-K^+K^-$, $2(K^+K^-)$, $\pi^+\pi^-p\overline{p}$, K_sK_s, $\phi\phi$, $\Lambda\overline{\Lambda}$ and $K^{\pm}K^0\pi^{\mp}$ final states. We find a number of discrepancies with the PDG values for these modes. We find no evidence for an $\eta_c(2S)$ with a mass near 3.594 GeV

1 Introduction

The BES experiment's sample of 3.5M ψ_{2S} decays provides an excellent opportunity to study $c\overline{c}$ charmonium particles. A major experimental issue for the charmonium particle aystem are the two charmonium states below open charm threshold that are still not well established: the $n = 2$ singlet S state, the $\eta_c(2S)$, and the $n = 1$ singlet P state, the $h_c(1P)$. The observation of these states and the determination of their mass would provide useful information on the spin-spin part of the charmonium potential.

The $\eta_c(2S)$ is expected to be produced in ψ_{2S} decays via the $M1$ radiative transition $\psi_{2S} \to \gamma\eta_c(2S)$. Transitions between the ψ_{2S} and the $h_c(1S)$ are forbidden and ψ_{2S} decays are not expected to be useful sources of this state. Here we report preliminary results from a search for the $\eta_c(2S)$ where the $\eta_c(2S)$ decays into four charged particles.

The Crystal Ball group [1] reported an excess of $E_\gamma \simeq 91$ MeV gamma rays from the inclusive $\psi_{2S} \to \gamma X$ process, and interpret this as possible evidence for the $\eta_c(2S)$ with mass 3.594 ± 0.005 GeV. This result has not been confirmed by any other experiment.

In the remainder of this section we briefly review the "conventional wisdom" about the $\eta_c(2S)$.

1.1 "Conventional wisdom"

1.1.1 The mass of $\eta_c(2S)$

The $\eta_c(2S)$ mass differs from that of the ψ_{2S} because of the hyperfine spin-spin interaction. In the simple potential model, the potential term for this splitting has the form [2]

$$H_{HFS} = \frac{16\pi\alpha_s}{9m_c^2}\ \vec{S_c}\cdot\vec{S_{\bar{c}}}\ \delta^3(\vec{r}), \tag{1}$$

where m_c is the c-quark mass and $\vec{S_c}$ is its spin vector. This gives a simple relation for the ratio of $\psi_{2S} - \eta_c(2S)$ and $J/\psi - \eta_c(1S)$ mass splitting:

$$\frac{\Delta M[\psi_{2S} - \eta_c(2S)]}{\Delta M[J/\psi - \eta_c(1S)]} \simeq \frac{\alpha_s(M_{\psi'})}{\alpha_s(M_{J/\psi})}\cdot\frac{|R_{2S}(0)|^2}{|R_{1S}(0)|^2}, \tag{2}$$

where the $R_{nS}(0)$ is the $c\bar{c}$ radial wavefunction at the origin. This can be evaluated from the ψ_{nS} leptonic width via the relation

$$\Gamma_{\psi_{nS}\to e^+e^-} = \frac{16\pi^2}{3}\alpha^2 e_c^2\frac{|R_{nS}(0)|^2}{M^2_{\psi_{nS}}}, \tag{3}$$

leading to the relation

$$M_{\psi'} - M_{\eta_c'} \simeq \frac{\alpha_s(M_{\psi'})}{\alpha_s(M_{J/\psi})}\cdot\frac{M^2_{\psi'}}{M^2_{J/\psi}}\cdot\frac{\Gamma_{\psi'\to e^+e^-}}{\Gamma_{J/\psi\to e^+e^-}}\cdot(M_{J/\psi} - M_{\eta_c}). \tag{4}$$

Using the PDG values for the masses and widths as summarized in Table 1 and $\alpha_s(M_{\psi'})/\alpha_s(M_{J/\psi}) = 0.9$, we find

$$M_{\psi'} - M_{\eta_c'} \simeq 65\text{MeV};\quad \text{i.e.}\quad M_{\eta_c'} \simeq 3.62\ \text{GeV}. \tag{5}$$

This calculation ignores binding effects and treats the quarks as being on-shell. The authors of ref. [2] note that using $M_\psi/2$ instead of m_c in eqn. 1 may be a better way to account for binding effects. In this case, this cancels the $(M_{\psi'}/M_{J/\psi})^2$ factor on the right-hand side of eqn. 4 reducing the expected splitting to ~ 47 MeV and raising $M_{\eta_c'}$ to 3.64 GeV. These mass estimates are substantially above the Crystal Ball group's reported mass value.

Table 1: A tabulation PDG values for the masses and widths of the $1S$ and $2S$ charmonium states.

Quantity	$1S$	$2S$
M_ψ	3096.88 ± 0.04 MeV	3686.00 ± 0.09 MeV
Γ_ψ^{tot}	87 ± 5 keV	277 ± 31 keV
$\Gamma_{\psi\to e^+e^-}$	5.2 ± 0.3 keV	2.3 ± 0.3 keV
M_{η_c}	2979.8 ± 2.1 MeV	3594 ± 5 MeV*
$\Gamma_{\eta_c}^{tot}$	$13.2^{+3.8}_{-3.2}$ MeV	< 8 MeV*
$\mathcal{B}(J/\psi \to \gamma\eta_c)$	$(1.3 \pm 0.4)\%$	$2.8 \pm 0.6 \times 10^{-3}$
$\Gamma_{\psi\to\gamma\eta_c(1S)}$	1.1 ± 0.4 keV	-

(* The PDG group does not include these results in their summary table.)

1.1.2 The branching fraction $\mathcal{B}[\psi_{2S} \to \gamma\eta_c(2S)]$

The $\psi_{2s} \to \gamma\eta_c(2S)$ process is an allowed $M1$ process with a width given by the relation [4]

$$\Gamma(\psi' \to \eta_c') = e_c^2\alpha(4k^3/3m_c^2)|I|^2(M_{\psi'}^2 + M_{\eta_c'}^2)/2M_{\psi'}^2, \tag{6}$$

where $e_c = 2/3$ is the c-quark charge, k is the photon momentum, and I is the initial-final state radial wavefunction overlap integral. With the exception of k, all of these factors are very nearly the same as for the $\psi_{1S} \to \gamma\eta_c(1S)$ transition, leading to the relation:

$$\mathcal{B}[\psi_{2S} \to \gamma\eta_c(2S)] = \frac{\Gamma(J/\psi \to \gamma\eta_c(1S))}{\Gamma_{tot}(\psi_{2S})} \cdot (\frac{k_{\eta_c'}}{k_{\eta_c}})^3 \simeq 2 \times 10^{-3}, \tag{7}$$

where the Crystal Ball value for the $\eta_c(2S)$ mass is used. For higher $\eta_c(2S)$ masses this reduces rapidly: for $M_{\eta_c'} = 3.62$GeV it decreases by a factor of three to $\mathcal{B} \simeq 7 \times 10^{-4}$; and for $M_{\eta_c'} = 3.64$GeV it decreases by a factor of eight to $\mathcal{B} \simeq 3 \times 10^{-4}$.

1.1.3 Expectations for $\eta_c(2S)$ decays

Like the $\eta_c(1S)$, the $\eta_c(2S)$ decays are expected to be dominated by hadronic modes mediated by $c\bar{c}$ annihilation into two-gluon intermediate states. The total width can be estimated from the relation

$$\Gamma^{tot}_{\eta'_c} \simeq \frac{\alpha_s(M_{\eta'_c})^2}{\alpha_s(M_{\eta_c})^2} \cdot \frac{|R_{2S}(0)|^2}{|R_{1S}(0)|^2} \Gamma^{tot}_{\eta_c} = \frac{\alpha_s(M_{\psi'})^2}{\alpha_s(M_{J/\psi})^2} \cdot \frac{M^2_{\psi'}}{M^2_{J/\psi}} \cdot \frac{\Gamma_{\psi' \to e^+e^-}}{\Gamma_{J/\psi \to e^+e^-}} \cdot \Gamma^{tot}_{\eta_c} \simeq = 8.1 \text{ MeV}. \quad (8)$$

This relatively large $\eta_c(2S)$ total width leads to the expectation that the relative rate for inter-charmonium transitions will be small. In this case, one expects that the branching fraction for $\eta_c(2S)$ to any specific hadronic final state will be the same as that for the corresponding $\eta_c(1S)$ decay [5].

1.2 Search strategy

In light of the above, a reasonable strategy for searching for the $\eta_c(2S)$ in the BES data is to concentrate on those decay modes that have been established for the $\eta_c(1S)$, which, according to the Particle Data Group [3], are:

$\eta_c(1S)$ decay final state	Branching fraction
$K\overline{K}\pi$	$(5.5 \pm 1.7)\%$
$K^{\pm}K_s\pi^{\mp}$	$(1.8 \pm 0.6)\%$
$\eta\pi\pi$	$(4.9 \pm 1.8)\%$
$K^+K^-K^+K^-$	$(2.1 \pm 1.2)\%$
$\pi^+\pi^-K^+K^-$	$(2.0 \pm 0.7)\%$
$\pi^+\pi^-\pi^+\pi^-$	$(1.2 \pm 0.4)\%$
$p\overline{p}$	$(1.2 \pm 0.4) \times 10^{-3}$

The $\psi_{2S} \to \gamma$ + four charged particles reaction is well suited for BES and covers many of the stategic decay modes. (For different $\eta_c(2S)$ mass values, the expected number of events will change as $(k_{\eta'_c}/91 \text{ MeV/c})^3$.)

1.2.1 Expectations

This analysis concentrates on searching for events of the type

$$\begin{aligned} \psi_{2S} &\to \gamma\chi_c; \\ \chi_c &\to h^+h^-h^+h^-, \end{aligned} \quad (9)$$

where h denotes either a π or K meson. From the above discussion and with values of the experimental acceptance (described in detail below), we can made the following estimates of the number of expected events in the BES data sample for a 3.594 GeV $\eta_c(2S)$:

$\eta_c(2S)$ decay final state	Branching fraction estimate	acceptance	expected number of events
$K^{\pm}K_s\pi^{\mp}$	4×10^{-5}	0.07*	10
$K^+K^-K^+K^-$	4×10^{-5}	0.09	12
$\pi^+\pi^-K^+K^-$	4×10^{-5}	0.14	15
$\pi^+\pi^-\pi^+\pi^-$	2.4×10^{-5}	0.14	11

*(Here the factor $\mathcal{B}(K_s \to \pi^+\pi^-) = 0.69$ is included.)

Since $\mathcal{B}[\psi_{2S} \to \gamma\eta_c(1S)] = (2.8 \pm 0.6) \times 10^{-3}$ is $\sim 40\%$ somewhat larger than the $\psi_{2S} \to \gamma\eta_c(2S)$ branching fraction used to estimate the number of events in the above table and the MC-determined acceptances for $\gamma\eta_c(1S)$ processes are typically $\sim 30\%$ higher, we expect to see nearly twice the number of $\eta_c(1S)$ events in each of these channels.

2 Event selection

We use all of the ψ_{2S} events on the four-prong data summary tapes. The corresponding number of ψ_{2S} decays is $N_{\psi_{2S}} = 3.44 \pm 0.3 \times 10^6$ [7]. We select events with four charged tracks with net charge zero and at least one γ's in the polar angle region $|\cos\theta| < 0.8$. We reject events where both the highest momentum positive and negative tracks are identified as muons or where both tracks have $E_{BHC} > 0.8$ GeV. Only those γ's with opening angles relative to each of the charged tracks in the event of 18^0 or more are considered. The events are subjected to four-constraint kinematic fits to the hypotheses $\psi_{2S} \to \gamma K^+K^-K^+K^-$, $\psi_{2S} \to \gamma\pi^+\pi^-K^+K^-$, $\psi_{2S} \to \gamma\pi^+\pi^-\pi^+\pi^-$, $\psi_{2S} \to \gamma K^{\pm}\pi^{\mp}K_s$; $K_s \to \pi^+\pi^-$, and $\psi_{2S} \to \gamma\pi^+\pi^-p\overline{p}$. In the case of events with more than one accepted gamma-ray candidate, the fits are applied for each gamma candidate and the one that gives the best fit is chosen. For the $\gamma K^{\pm}\pi^{\mp}K_s$ mode, the $K_s \to \pi^+\pi^-$ track candidates are required to pass the KLAMSLOW secondary vertexing routine and the K_s invariant mass is included in the kinematic fit as a fifth constraint.

For each particular channel, the confidence level of the kinematic fit is required to be larger than 0.05 and also larger than that the confidence level for the fit to any of the other considered modes. We reject events where the mass recoiling against any $\pi^+\pi^-$ pair is within ± 50 MeV of $M_{J/\psi}$. For the $\pi^+\pi^-\pi^+\pi^-$ ($\pi^+\pi^-K^+K^-$) mode we reject events where the $\pi^+\pi^-$ pairs have (pair has) an invariant mass within ± 20 MeV of M_{K_s}. For the $K^{\pm}K_s\pi^{\mp}$ mode we require a good vertex fit from KLAMSLOW with $c\tau > 5.0$ mm. Backgrounds to this channel from misidentified $\chi \to K_sK_s$ are eliminated by

Table 2: A tabulation of the $\psi_{2S} \to \gamma h^+h^-h^+h^-$ selection cuts.

The number of events surviving each requirement

	$K^+K^-K^+K^-$	$\pi^+\pi^-K^+K^-$	$\pi^+\pi^-\pi^+\pi^-$	$K^\pm K_s\pi^\mp$	$\pi^+\pi^-p\overline{p}$
4 chrgd trks					
$\sum q = 0$					
$N_\gamma \geq 1$	820256				
$N_\mu < 2$	808334				
$N_{e^+,e^-} < 2$	780888				
$\lvert\cos\theta_{trk}\rvert < 0.8$	545920				
$\theta_{\gamma-trk} > 18^0$	530147				
$\lvert\cos\theta_\gamma\rvert < 0.8$					
χ^2 cuts (see text)	2746	7186	5820	1365	12336
$\lvert M_{\pi\pi}^{recoil} - M_{J/\psi}\rvert > 0.05$ GeV	-	5938	3495	932	9867
$\lvert M_{\pi\pi} - M_{K_s}\rvert > 0.02$ GeV	-	5618	3007	-	-
$K_s \to \pi^+\pi^-$ cuts	-	-	-	363	-
$M_{K^\pm\pi^\mp} > 0.85$GeV	-	-	-	289	-
Particle id cuts	217	1736	2618	173	402

requiring $M_{K^\pm\pi^\mp} > 0.85$GeV. We use the dE/dx and TOF routines recently developed Dunwoodie and Li [8] to compute combined, four-track particle i.d. confidence levels for each event hypothesis. For each decay channel, we require the confidence level for the dE/dx *or* the TOF systems to be greater than 0.05.

A summary of the number of events that pass each selection criterion for each mode is listed in Table 2.

3 Results

3.1 $\psi_{2S} \to \gamma K^+K^-K^+K^-$

Figure 1 shows the four kaon mass distribution from selected $\psi_{2S} \to \gamma K^+K^-K^+K^-$ events. Peaks at the position of the three ^3P charmonium states, $\chi_{0,1,2}$, are evident. There are only three events in the $\eta_c(1S)$ mass region, where we expect more than 12, leading us to suspect the PDG branching ratio value, which is based only on a single measurement [9]. The solid curve indicates the results of a fit using four Breit Wigner functions convoluted with a gaussian resolution function to represent the $\eta_c(1s)$ and the $\chi_{0,1,2}$ charmonium states, and a third order polynomial background function. The widths of the charmonium states are fixed at their measured values and the masses are left as free parameters. The fit masses are consistent with their established values.

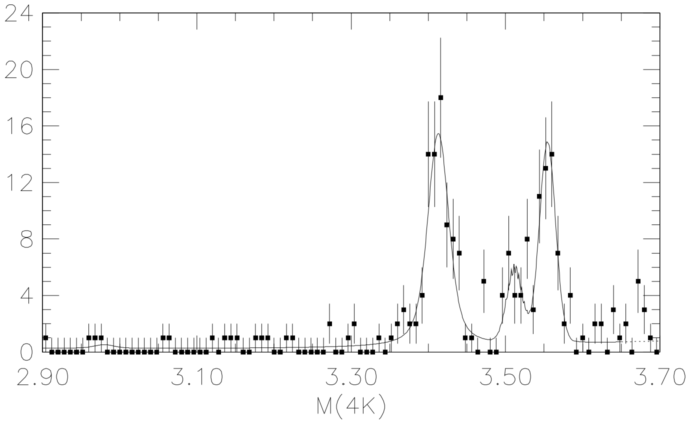

Figure 1: The four kaon invariant mass distribution from selected $\psi_{2S} \rightarrow \gamma K^+K^-K^+K^-$ events. The curve indicates the results of a fit to the spectrum that includes the $\eta_c(1S)$, the three ^3P charmonium states and a third-order polynomial background.

The data in Fig. 1 are well fit by the four-resonance hypothesis and there is no evidence for an $\eta_c(2S)$ signal near 3.6 GeV, certainly not at the expected 14-event level as discussed above. Figure 2 shows the results of a fit with a $\Gamma_{tot} = 8.1$MeV Breit-Wigner function with mass constrained to between 3.59 and 3.61 GeV. In order to maximize a possible $\eta_c(2S)$ contribution, we do not include any background function. This fit gives 4.6 ± 3.6 events in this additional peak. Since the overall confidence level is worse with the the additional peak than without it, we use the measured number of events to infer a 90% confidence level upper limit of 9.2 events.

We summarize the numbers of $K^+K^-K^+K^-$ events for each of the charmonium states below. Here only statistical errors are included.

N_{η_c}	N_{χ_0}	N_{χ_1}	N_{χ_2}	$N_{\eta_c'}$
1.3 ± 2.9	72 ± 10	15 ± 5	41 ± 7	< 9.2 (90% CL)

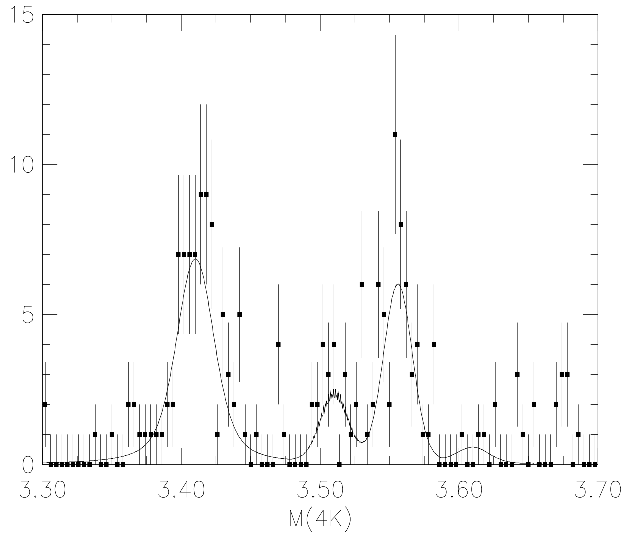

Figure 2: The four kaon invariant mass distribution fit with an additional Breit-Wigner function with a total width fixed at 8.1 MeV and a mass allowed to range between 3.59 and 3.61 GeV.

As noted above, the absence of an $\eta_c(1S)$ of any significance in this mode leads one to suspect the PDG value for the $\eta_c \to K^+K^-K^+K^-$ branching fraction and, thus, the usefulness of this channel for an $\eta_c(2S)$ search.

3.1.1 $\psi_{2S} \to \gamma\phi\phi$

Figures 3a and b show $M_{K^+K^-}$ *vs* $M_{K^+K^-}$ scatterplots for events with four-kaon masses consistent with the χ_0 and χ_2, respectively. In both plots, there are clusters of events in the lower left corner corresponding to $\chi_{0,2} \to \phi\phi$ decays. The $\chi_1 \to \phi\phi$ process violates the Yang rule and is expected to be suppressed.

Figure 4 shows the four-kaon mass distribution for events where both K^+K^- pairs have an invariant mass within 20 MeV of M_ϕ. Peaks occur at the location of the χ_0 and the χ_2. There is one event at the location of the χ_1 and one event at the $\eta_c(1S)$ (off scale in Fig. 4). This distribution is fit with two resolution-convoluted Breit Wigner functions with events yields of $N_{\chi_0} = 11 \pm 5$ and $N_{\chi_2} = 13 \pm 4$.

3.2 $\psi_{2S} \to \gamma\pi^+\pi^-K^+K^-$

Figure 5 shows the $\pi^+\pi^-K^+K^+$ mass distribution from the selected events. Prominent peaks at the position of the three ${}^3P$ charmonium states, $\chi_{0,1,2}$, are evident, and there is some excess in the region of the $\eta_c(1S)$.

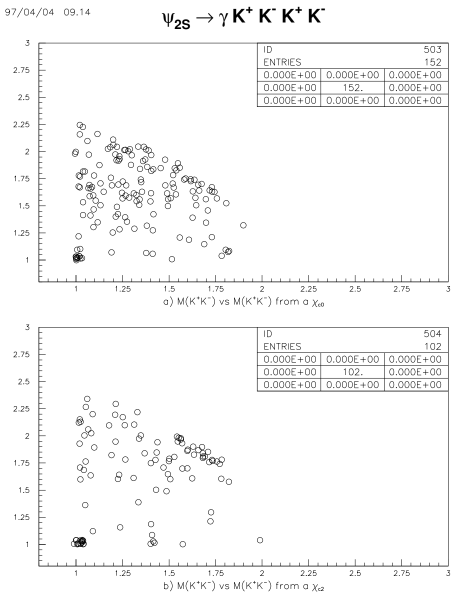

Figure 3: The $M_{K^+K^-}$ *vs* $M_{K^+K^-}$ scatterplot for four kaon masses in the **a)** χ_0 and **b)** χ_2 regions.

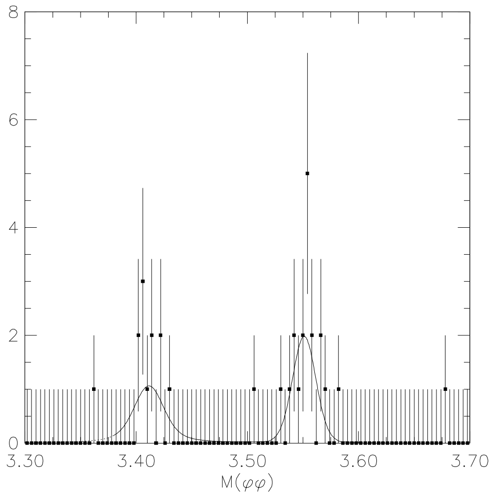

Figure 4: Fit to the $\phi\phi$ mass distribution.

The solid curve indicates the results of a fit using four Breit Wigner functions convoluted with a gaussian resolution function and a fifth-order polynomial background function. The widths of the charmonium states are fixed at their measured values and the masses are left as free parameters, The masses given by the fit are consistent with their established values. The η_c peak consists of 34 ± 8 events, which is near the expected level.

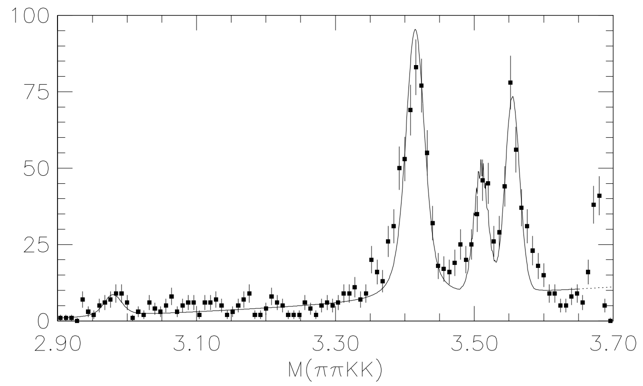

Figure 5: The $\pi^+\pi^-K^+K^-$ invariant mass distribution. The curve indicates the results of a fit to the spectrum that includes the $\eta_c(1S)$, the three ^3P charmonium states and a fifth-order polynomial background.

There is no evidence in Fig. 5 for an $\eta_c(2S)$ signal at 3.6 GeV. Including a Breit Wigner function with area fixed at 15 events, width fixed at 8.1 MeV, and a mass free to range between 3.59 and 3.61 GeV improves the confidence level of the fit, but only marginally. There is, however, some excess of events on the high mass side of the $\chi_{c2}(3556)$ peak. We repeated the fit with an additional narrow Breit Wigner function with mass constrained to between 3.57 and 3.62 GeV and a total width fixed at 8.1 MeV. This fit, shown in Fig. 6 likes a rather signal of 36 events at a mass of 3.582GeV. This could be due to feedthrough from $\chi_2 \to 4\pi$ decays, although Monte Carlo simulations indicate that this feedthrough should be small. This requires further investigation.

We summarize the numbers of events for each of the charmonium states seen in the $\pi^+\pi^-K^+K^-$ channel in the chart below. In this chart, the numbers for the $\chi_{0,1,2}$ are taken from a fit to the distribution of Fig. 6 without a fourth Breit Wigner function. Here only statistical errors are included.

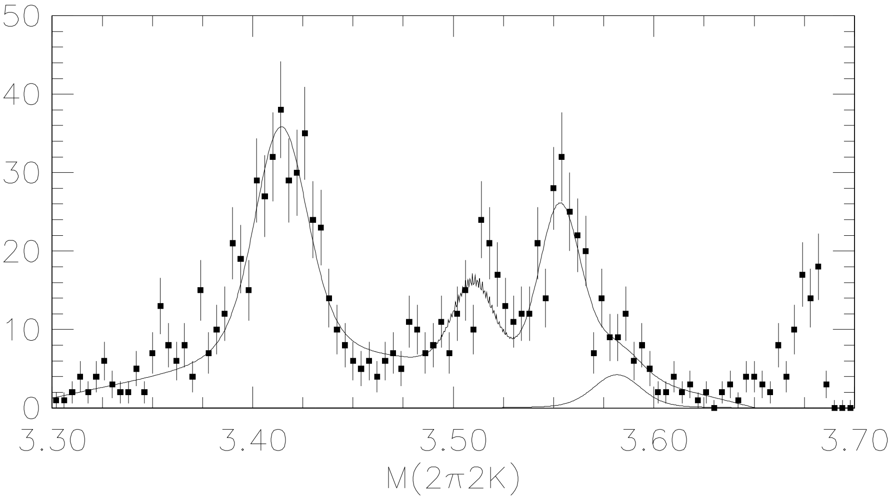

Figure 6: The $\pi^+\pi^-K^+K^-$ invariant mass distribution fit to four Breit-Wigner functions and a fifth-order polynomial background.

N_{η_c}	N_{χ_0}	N_{χ_1}	N_{χ_2}
34 ± 8	438 ± 28	126 ± 16	212 ± 19

3.3 $\psi_{2S} \to \gamma\pi^+\pi^-\pi^+\pi^-$

Figure 7 shows the four pion mass distribution from selected $\psi_{2S} \to \gamma\pi^+\pi^-\pi^+\pi^-$ events. Prominent peaks at the position of the three ^3P charmonium states, $\chi_{0,1,2}$, are evident, and there is some excess in the region of the $\eta_c(1S)$.

The solid curve indicates the results of a fit using four Breit Wigner functions convoluted with a gaussian resolution function and a fifth-order polynomial background function. The widths of the charmonium states are fixed at their measured values and the masses are left as free parameters, The masses given by the fit are consistent with their established values. Here, although the signal-to-noise at the $\eta_c(1S)$ is poor, the data are consistent with an η_c signal at around the expected level.

There is no evidence in Fig. 7 for an $\eta_c(2S)$ signal at 3.6 GeV. Including a Breit Wigner function with area fixed at 11 events, width fixed at 8.1 MeV, and a mass free to range between 3.59 and 3.61 GeV increases χ^2 by 2.4 units. As in the case of the $\pi^+\pi^-K^+K^-$ channel, there is some excess of events on the high mass side of the $\chi_{c2}(3556)$ peak. We repeated the fit with an additional narrow Breit Wigner function with mass constrained to between 3.57 and 3.62 GeV and a total width fixed at 0.001 GeV. This fit, shown in Fig. 8 likes a rather substantial signal of 117 events

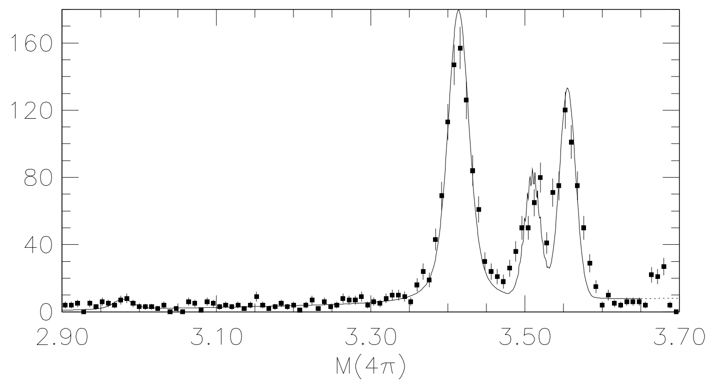

Figure 7: The four pion invariant mass distribution from selected $\psi_{2S} \to \gamma\pi^+\pi^-\pi^+\pi^-$ events. The curve indicates the results of a fit to the spectrum that includes the $\eta_c(1S)$, the three ^3P charmonium states and a fifth-order polynomial background.

at a mass of 3.570GeV. The fitted fourth BW mass tends to be as close to $M_{\chi_2(3556)}$ as is allowed and there is a potential for significant feedthrough from the χ_2.

We summarize the numbers of events for each of the charmonium states seen in the four pion channel in the chart below. In this chart, the numbers for the $\chi_{0,1,2}$ are taken from a fit to the distribution of Fig. 8 without a fourth Breit Wigner function. Here only statistical errors are included

N_{η_c}	N_{χ_0}	N_{χ_1}	N_{χ_2}
29 ± 8	772 ± 34	189 ± 18	396 ± 24

3.3.1 $\psi_{2S} \to \gamma K_s K_s$

Figures 9a and b show $M_{\pi\pi}$ *vs* $M_{\pi\pi}$ scatterplots for events with four-pion masses consistent with the χ_0 and χ_2, respectively. In both plots, there are clusters of events in the lower left corner corresponding to $\chi_{0,2} \to K_s K_s$ decays. (These clusters are excluded from the $\chi \to 4\pi$ analysis described above.) The decay $\chi_1 \to K_s K_s$ is forbidden by parity.

Figure 10 shows the four-pion mass distribution for events where both $\pi^+\pi^-$ pairs have an invariant mass within 20 MeV of M_{K_s}. Peaks occur at the location of the χ_0 and, possibly, the χ_2. This distribution is fit with two resolution-convoluted Breit Wigner functions with events yields of $N_{\chi_0} = 36 \pm 8$ and $N_{\chi_2} = 6 \pm 4$.

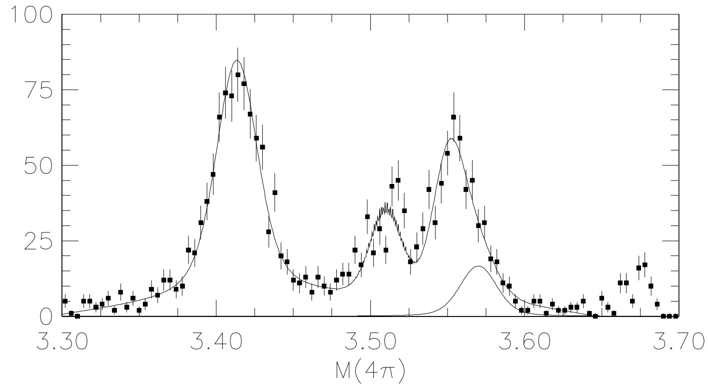

Figure 8: The four pion invariant mass distribution fit to four Breit-Wigner functions and a fifth-order polynomial background.

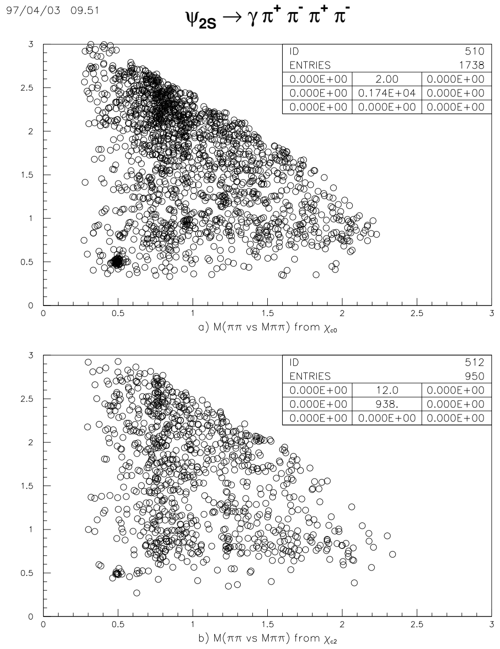

Figure 9: The $M_{\pi^+\pi^-}$ *vs* $M_{\pi^+\pi^-}$ scatterplot for four pion masses in the **a)** χ_0 and **b)** χ_2 regions.

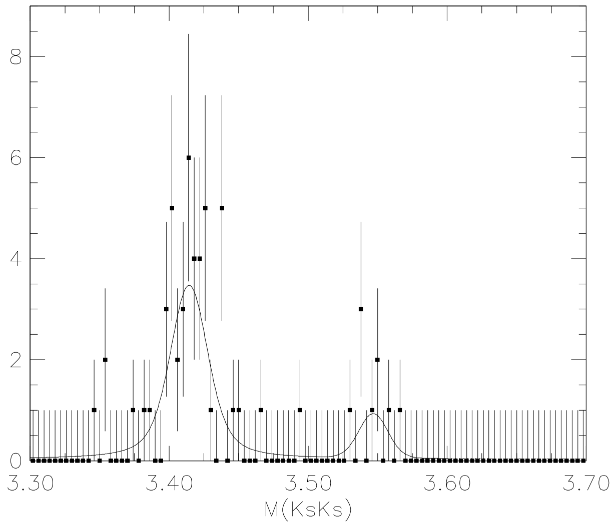

Figure 10: Fit to the K_sK_s mass distribution.

3.4 $\psi_{2S} \to \gamma K^{\pm} K_s \pi^{\mp}$

Since neither the ψ_{2S} nor the χ_2 have strong decays to $K\overline{K}\pi$, this channel is, perhaps, the most promising mode for the $\eta_c(2S)$, particularly if it is near the mass of the χ_2 as may be indicated by the $\pi\pi KK$ and 4π data. Even though the number of events expected for this channel is low (i.e. ~ 10), backgrounds are low and the $K_s \to \pi^+\pi^-$ decay provides for excellent particle identification. (If the $\eta_c(2S)$ mass is around 3.58 GeV as indicated by the $\pi\pi KK$ and 4π data, the expected number of $KK\pi$ events should be increased by a factor of 1.6 to ~ 16 events.

Figure 11 shows the $KK\pi$ mass distribution from selected $\psi_{2S} \to \gamma K^{\pm} K_s \pi^{\mp}$ events. A peak at the positions of the χ_1 is evident and there is some indication of signals for the $\eta_c(1S)$ and the χ_2. The solid curve indicates the results of a fit using four Breit Wigner functions convoluted with a gaussian resolution function to represent the charmonium states, and a third order polynomial background function. The widths of the charmonium states are fixed at their measured values. The masses of the charmonium states, left as free parameters in the fit, are all consistent with their established values.

There is no evidence in Fig. 11 for an $\eta_c(2S)$ signal near 3.6 GeV. This is illustrated in Fig. 12, where we show the results of a fit with an additional narrow Breit Wigner function with mass constrained to between 3.59 and 3.60 GeV, a total width fixed at 8.1 MeV. The fit gives this additional resonance a total area of 0.9 ± 3.3 events. Since a fit without an additional resonance has an improved confidence level, we use this result to determine a 90% confidence upper limit of six events. Fits with the mass of

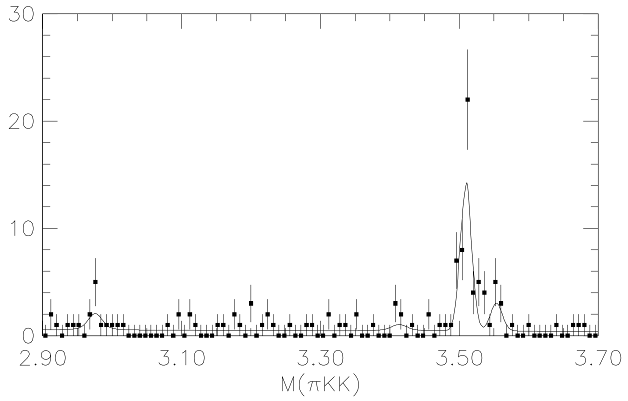

Figure 11: The $KK\pi$ invariant mass distribution from selected $\psi_{2S} \rightarrow \gamma K^{\pm}K_s\pi^{\mp}$ events. The curve indicates the results of a fit to the spectrum that includes the three ^3P χ states, the $\eta_c(1S)$ and a third-order polynomial background.

the extra resonance allowed to be lower results in a somewhat larger number of events: if the mass is allowed to go as low as 3.57 GeV, the area of the extra peak increases to 4.7 ± 3.9 events. However the confidence level is still better for the fit with no additional resonance.

We summarize the numbers of events in the Breit-Wigner peaks for the $KK\pi$ mass spectrum of Fig. 11 in the chart below. Here only statistical errors are included.

N_{η_c}	N_{χ_0}	N_{χ_1}	N_{χ_2}	$N_{\eta_c'}$
5.9 ± 3.9	< 10	31.4 ± 6.0	6.1 ± 3.4	< 6 (90% CL)

3.5 $\psi_{2S} \rightarrow \gamma\pi^+\pi^-p\overline{p}$

Figure 13 shows the $\pi^+\pi^-p\overline{p}$ mass distribution for selected events. Peaks at the positions of the three χ states are evident and there are no indications of an η_c nor of an $\eta_c(2S)$. Fitting the spectrum gives the following numbers of events for each χ state:

N_{χ_0}	N_{χ_1}	N_{χ_2}
102 ± 12	25 ± 6	70 ± 9

Figure 14 shows the $M_{p\pi^-}$ *vs* $M_{\overline{p}\pi^+}$ scatterplot for selected $\pi\pi p\overline{p}$ events. Here no particle identification cuts are used. A cluster of events indicating $\chi \rightarrow \Lambda\overline{\Lambda}$ is evident in the lower left hand corner.

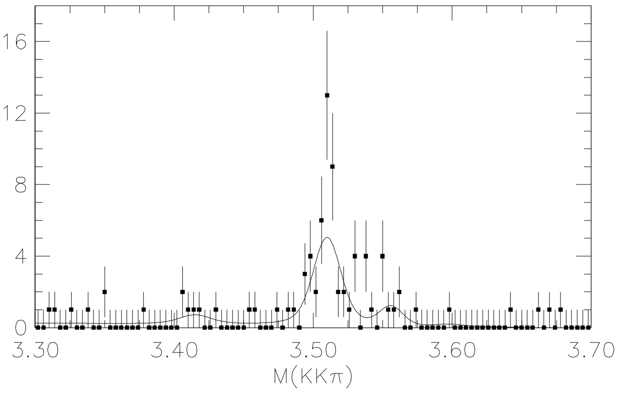

Figure 12: The $KK\pi$ invariant mass distribution fit with an additional Breit Wigner with a total width of 8.1 MeV and a mass constrained to be between 3.59 and 3.61 GeV.

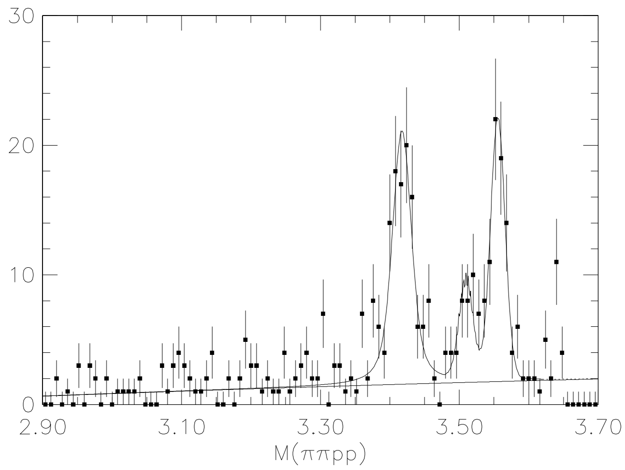

Figure 13: The $\pi^+\pi^- p\overline{p}$ invariant mass distribution. The curve indicates the results of a fit to the spectrum that includes the three ^3P charmonium states and a second-order polynomial background.

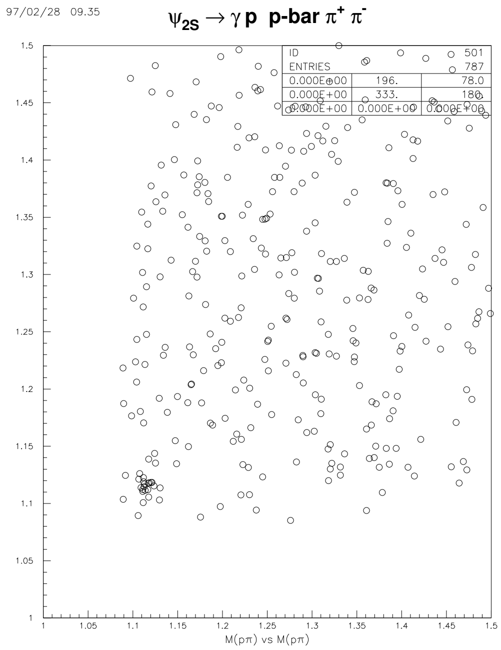

Figure 14: The $M_{p\pi^-}$ vs $M_{\overline{p}\pi^+}$ scatterplot.

These events were reprocessed through the KLAMSLOW secondary vertexing routine and events where both the Λ and $\overline{\Lambda}$ candidates are found to have a $c\tau$ greater than 3 cm are selected. Figure 15 shows the $\pi^+\pi^-p\overline{p}$ mass distribution for events where both $p\pi$ pairs have an invariant mass within 30 MeV of M_Λ. The events cluster at the location of the χ_0 and χ_2, and, possibly the χ_1. Fitting this distribution is fit with three resolution-convoluted Breit Wigner functions yields event numbers of $N_{\chi_0} = 5.5 \pm 3.6$, $N_{\chi_1} = 2.7 \pm 2.3$ and $N_{\chi_2} = 5.7 \pm 2.7$.

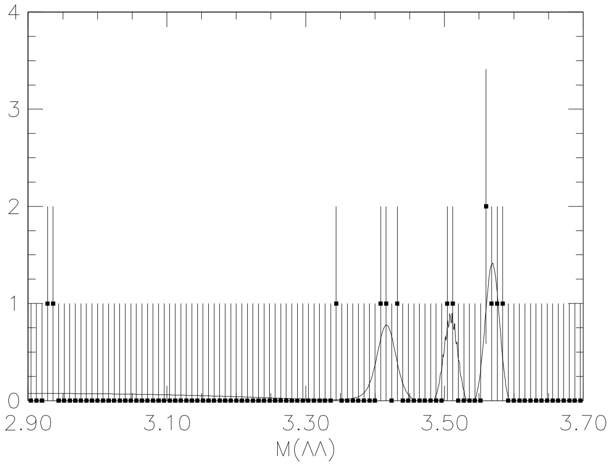

Figure 15: Fit to the $\Lambda\overline{\Lambda}$ mass distribution.

3.6 Acceptance

To determine the acceptance, we generated samples of 1000 simulated Monte Carlo events for each of the decay channels that were investigated. For the $\psi_{2S} \to \gamma(c\bar{c})$ transition, we use the following angular distributions [10]:

$(c\bar{c})$	$dN/d\cos\theta$
$\eta_c(1S)$	$1+\cos^2\theta$
χ_{c0}	$1+\cos^2\theta$
χ_{c1}	$1-0.18\cos^2\theta$
χ_{c2}	$1+0.08\cos^2\theta$
$\eta_c(2S)$	$1+\cos^2\theta$

To investigate the dependence of the acceptance on the resonant structure of the four particle final states, we generated $(c\bar{c})$ decays via a variety of two and three-body meson resonance states. The number of events from each simulated event sample that are detected and survive the selection criteria are given in Table 3. In the K_s modes, all of the K_s' are decayed to $\pi^+\pi^-$; likewise for $\Lambda \to p\pi^-$. These acceptances do not include the efficiency of the particle identification cuts that have not yet been properly implemented in the BES simulation program. For the time being, I take this efficiency to be $(90 \pm 5)\%$ based on their observed effects on the number of events in the $\psi_{2S} \to \omega\pi\pi$, $\chi_0 \to K_sK_s$, and $\chi_2 \to \phi\phi$, event samples, where very clean signals are seen without the application of any particle identification requirements.

3.7 Branching ratio determinations

The $\eta_c(1S)$ and $\chi_{0,1,2}$ branching ratios to each of the channels being investigated are determined from the relation

$$\mathcal{B}(\chi_i \to h^+h^-h^+h^-) = \frac{N_{evts}(\chi_i)}{N_{\psi_{2S}}\mathcal{B}(\psi_{2S} \to \gamma\chi_i)\eta}, \tag{10}$$

where η is the acceptance and the branching fractions $\mathcal{B}(\psi_{2S} \to \gamma(c\bar{c})$, taken from the PDG tables, are

	$\eta_c(1S)$	χ_0	χ_1	χ_2
$\mathcal{B}(\psi_{2S} \to \gamma\chi_i)$	0.0028 ± 0.0006	0.093 ± 0.008	0.087 ± 0.008	0.078 ± 0.008

Table 3: A tabulation of the number of simulated events from different decay generators that survive the event selection process. In each case, the number of generated events is 1000.

	$\eta_c(1S)$	χ_{c0}	χ_{c1}	χ_{c2}	$\eta_c(2S)$
$\pi^+\pi^-\pi^+\pi^-$		149			
$\rho\pi^+\pi^-$					
$a_1^+\pi^-$		147			
$\rho\rho$				191	158
$K^+K^-\pi^+\pi^-$					
$K^*K^+\pi^-$		156			
$K_1(1270)K^-$					
$K^+K^-K^+K^-$					
ϕK^+K^-	99				82
$\phi\phi$				281	
$K^+K_s\pi^-$	109		89		80
K_sK_s		112			
$\pi^+\pi^-p\overline{p}$		176			
$\Lambda\overline{\Lambda}$		190			

3.7.1 $\mathcal{B}(K^+K^-K^+K^-)$ measurements

$\boldsymbol{\mathcal{B}(\chi \to \phi\phi)}$**:** The process $\chi \to \phi\phi \to K^+K^-K^+K^-$ leads to final states with very nearly back-to-back K^+K^- pairs with nearly equal momentum. As is apparent in Table 3, this event topology has a dramatically higher acceptance than other four-kaon processes. We treat these decays separately.

The $\chi_{0,2} \to \phi\phi$ branching fractions are determined using using the relation in eqn. 10 with $\eta = 0.25 \pm 0.03$ and an additional factor of $\mathcal{B}^2(\phi \to K^+K^-) = 0.241 \pm 0.006$ [3] in the denominator to account for the fact that only charged decays are included in the acceptance calculation. The results:

	χ_0 $(\times 10^{-3})$	χ_2 $(\times 10^{-4})$
$\mathcal{B}(\chi \to \phi\phi)$	5.7 ± 2.5	8.2 ± 2.5
C.Z.Yuan values	8.3 ± 3.7	18.2 ± 5.6

are below those of Yuan. The discrepancy between our measurements lies in the acceptance calculation. Yuan uses an acceptance of 0.1, which is very low considering the simple topology of these events. There are no PDG listings for these decays.

$\boldsymbol{\mathcal{B}(K^+K^-K^+K^-)}$**:** The results for the $4K$ decays, are summarized in Table 4. Here, the χ_0 and $\chi_2 \to \phi\phi$ decays are treated separately as discussed above and the acceptance values listed in the Table are for the non-$\phi\phi$ component of the $4K$ final states. The 90% CL upper limit $\mathcal{B}(\eta_c(1s) \to K^+K^-K^+K^-) < 4.8 \times 10^{-3}$ contrasts with the PDG value of $2.1 \pm 1.2)$%. There are no PDG entries for this channel for the χ states. The numbers are in good agreement with those determined by Yuan [12].

Table 4. Branching fractions for $K^+K^-K^+K^-$ final states.

	$\eta_c(1S)$	χ_0	χ_1	χ_2
N_{evts} (non-$\phi\phi$)	< 4	61 ± 10	15 ± 5	28 ± 7
η	0.09 ± 0.01	0.09 ± 0.01	0.09 ± 0.01	0.09 ± 0.01
$\mathcal{B}(4K\ \mathrm{non} - \phi\phi) \times 10^{-3}$	< 4.8	2.1 ± 0.6	0.6 ± 0.2	1.2 ± 0.3
$\mathcal{B}(\phi\phi \to K^+K^-K^+K^-) \times 10^{-3}$	-	0.14 ± 0.06	-	0.20 ± 0.06
$\mathcal{B}(K^+K^-K^+K^-) \times 10^{-3}$	< 4.8	2.2 ± 0.6	0.6 ± 0.2	1.4 ± 0.3
C.Z. Yuan values $(\times 10^{-3})$	-	2.7 ± 0.5	0.4 ± 0.2	1.6 ± 0.4
PDG values $(\times 10^{-3})$	21 ± 12	–	–	–

We use the upper limit of 9.2 events for a resonance in the 3.59 to 3.61 GeV mass interval together with an estimated acceptance value of $\eta = 0.08$ to establish a 90%

CL upper limit for an $\eta_c(2S)$ with a mass consistent with the PDG value:

$$\mathcal{B}(\psi_{2S} \to \gamma\eta_c(2S)) \times \mathcal{B}(\eta_c(2S) \to K^+K^-K^+K^-) < 3.3 \times 10^{-5} \quad (90\%\mathrm{CL}) \qquad (11)$$

3.7.2 $\mathcal{B}(\pi^+\pi^-K^+K^-)$ measurements

The results for the $2\pi 2K$ decays are summarized in Table 5. Here the acceptance for χ_2 decays is increased slightly relative to the others because of a stronger contribution of $\chi_2 \to K^*\overline{K^*}$ [13]. While our result for the $\eta_c(1S)$ agrees within errors with the PDG entry for this mode, our results for the χ_c states are consistently about a factor of three lower. The PDG entries for these decays are based on a single experiment, that by the Mark-I group [14]. Our results for the χ states are consistently about 50% below Yuan's results. This may be due to differences in the particle identification.

Table 5. Branching fractions for $\pi^+\pi^-K^+K^-$ final states.

	$\eta_c(1S)$	χ_0	χ_1	χ_2
N_{evts}	34 ± 6	438 ± 28	126 ± 16	212 ± 19
η	0.14 ± 0.02	0.14 ± 0.02	0.14 ± 0.01	0.17 ± 0.02
$\mathcal{B}(\pi^+\pi^-K^+K^-) \times 10^{-2}$	2.5 ± 0.8	0.99 ± 0.21	0.30 ± 0.07	0.46 ± 0.10
C.Z. Yuan values ($\times 10^{-2}$)	-	1.42 ± 0.27	0.46 ± 0.09	0.79 ± 0.17
PDG values ($\times 10^{-2}$)	$2.0^{+0.7}_{-0.6}$	3.0 ± 0.7	0.9 ± 0.4	1.9 ± 0.5

3.7.3 $\mathcal{B}(\pi^+\pi^-\pi^+\pi^-)$ measurements

The results for the 4π decays are summarized in Table 6. Here the acceptance for χ_2 decays is increased slightly relative to the others because of a stronger contribution of $\chi_2 \to \rho\rho$ [13], which has a somewhat higher acceptance than the $a_1\pi$ mode that appears to be dominant for the χ_0. Our result for the $\eta_c(1S)$ is in reasonable agreement with the PDG value for this channels, but our results for the χ_c states are substantially below the PDG values. The pattern is similar to that seen for the $2\pi 2K$ decay mode and the PDG entries are based entirely on the same Mark-I measurement [14]. Our measurements for the χ states agree well with those of Yuan.

Table 6. Branching fractions for $\pi^+\pi^-\pi^+\pi^-$ final states.

	$\eta_c(1S)$	χ_0	χ_1	χ_2
N_{evts}	29 ± 8	772 ± 34	189 ± 18	396 ± 24
η	0.14 ± 0.02	0.14 ± 0.02	0.14 ± 0.01	0.17 ± 0.02
$\mathcal{B}(\pi^+\pi^-\pi^+\pi^-) \times 10^{-2}$	2.0 ± 0.7	1.72 ± 0.35	0.45 ± 0.10	0.87 ± 0.18
C.Z. Yuan values ($\times 10^{-2}$)	-	1.56 ± 0.24	0.48 ± 0.09	1.01 ± 0.17
PDG values ($\times 10^{-2}$)	1.2 ± 0.4	3.7 ± 0.7	1.6 ± 0.5	2.2 ± 0.5

$\mathcal{B}(K_s K_s)$: The $\chi_{0,2} \to K_s K_s$ branching fractions are determined using using the relation in eqn. 10 with $\eta = 0.11 \pm 0.01$ and an additional factor of $\mathcal{B}^2(K_s \to \pi^+\pi^-) = 0.471 \pm 0.004$ [3] in the denominator to account for the fact that only charged decays are included in the acceptance calculation. The results:

	χ_0 ($\times 10^{-3}$)	χ_2 ($\times 10^{-3}$)
$\mathcal{B}(\chi \to K_s K_s)$	2.2 ± 0.6	0.4 ± 0.3
C.Z.Yuan values	2.4 ± 0.4	0.5 ± 0.2
PDG: $1/2\mathcal{B}(\chi \to K^+K^-)$	3.5 ± 1.2	0.7 ± 0.5

agree well with those of Yuan. Although there are no PDG listings for $\chi \to K_s K_s$, our results agree within errors with the ispin expectations applied to DASP results for K^+K^- decays [15].

3.7.4 $\mathcal{B}(K^\pm K_s \pi^\mp)$ measurements

The results for the $KK\pi$ decays are summarized in Table 7. Here the acceptance for includes the factor $\mathcal{B}(K_s \to \pi^+\pi^-) = 0.69$. Our result for the η_c agrees within errors with the PDG value for this mode. These are no PDG entries for χ decays to this channel. Our results agree with those of Yuan, although we quote a 2σ branching ratio for the χ_2, while Yuan provides an upper limit.

Table 7. Branching fractions for $K^\pm K_s \pi^\mp$ final states.

	$\eta_c(1S)$	χ_0	χ_1	χ_2
N_{evts}	5.9 ± 3.9	< 10	31.4 ± 6.0	6.0 ± 3.4
η	0.06 ± 0.01	0.054 ± 0.01	0.054 ± 0.01	0.054 ± 0.01
$\mathcal{B}(K^\pm K_s \pi^\mp)(\times 10^{-2})$	1.0 ± 0.6	< 0.06	0.19 ± 0.06	0.041 ± 0.025
C.Z. Yuan values ($\times 10^{-2}$)	-	< 0.08	0.25 ± 0.07	< 0.13
PDG values ($\times 10^{-2}$)	1.8 ± 0.6	–	–	–

We use the upper limit of 6 events in the 3.59 to 3.61 GeV mass interval and an acceptance value of $\eta = 0.06$ to establish a 90% CL upper limit for an $\eta_c(2S)$ with a mass consistent with the PDG value:

$$\mathcal{B}(\psi_{2S} \to \gamma\eta_c(2S)) \times \mathcal{B}(\eta_c(2S) \to K^{\pm}K_s\pi^{\mp}) < 3.0 \times 10^{-5} \;\; (90\%\text{CL}). \qquad (12)$$

3.7.5 $\mathcal{B}(\pi^+\pi^-p\overline{p})$ measurements

The results for the $\chi \to \pi\pi p\overline{p}$ decays are summarized in Table 8. Here the acceptance is taken from a simulation of $\chi_0 \to \pi\pi p\overline{p}$ decays generated with a four-body phase-space distribution. Our results agree with Yuan's and are substantially below the PDG values. The pattern is similar to that seen for the $2\pi 2K$ and 4π decay modes and the PDG entries are based entirely on the same Mark-I measurement [14].

Table 8. Branching fractions for $\pi^+\pi^-p\overline{p}$ final states.

	χ_0	χ_1	χ_2
N_{evts}	102 ± 12	25 ± 6	70 ± 9
η	0.16 ± 0.02	0.16 ± 0.02	0.16 ± 0.02
$\mathcal{B}(\pi^+\pi^-p\overline{p})(\times 10^{-3})$	1.9 ± 0.3	0.5 ± 0.2	1.6 ± 0.4
C.Z. Yuan values ($\times 10^{-3}$)	1.6 ± 0.4	0.35 ± 0.18	1.3 ± 0.4
PDG values ($\times 10^{-3}$)	5.0 ± 2.0	1.4 ± 0.9	3.3 ± 1.3

$\mathcal{B}(\Lambda\overline{\Lambda})$ measurements The $\chi_{0,1} \to \Lambda\overline{\Lambda}$ branching fractions are determined using using the relation in eqn. 10 with $\eta = 0.19 \pm 0.01$ and an additional factor of $\mathcal{B}^2(\Lambda \to p\pi^-) = 0.408 \pm 0.006$ [3] in the denominator to account for the fact that only charged decays are included in the acceptance calculation. The results are:

	χ_0	χ_1	χ_2
$\mathcal{B}(\chi \to \Lambda\overline{\Lambda}) \times 10^{-4}$	2.2 ± 1.5	1.2 ± 1.0	2.7 ± 1.3

Yuan has not reported any results for $\chi \to \Lambda\overline{\Lambda}$ and there are no PDG entries for this channel.

4 Summary and Discussion

A search of ψ_{2S} decays to $\gamma h^+h^-h^+h^-$ final states indicates no evidence for an $\eta_c(2S)$ at a mass near the Crytsal Ball value. Unfortunately, the sensitivity of the search is around the expected event rate in each channel. Nevertheless, the absence of a compelling signal in any of the four channels under investigation, leads one to question the reliability of the Crystal Ball result.

Both the $2(\pi^+\pi^-)$ and the $\pi^+\pi^-K^+K^-$ channels show peculiar shoulders on the high mass side of the χ_2 peak. There are no enhancements in the $2(K^+K^-)$ and the $K^\pm K_s\pi^\mp$ distributions in the same mass region. Moreover, the events in the shoulders appear very similar to those near the χ_2 peak: in both mass ranges the 4π channel shows a strong $\rho\rho$ signal and the $2\pi 2K$ channel is dominated by $K^*\overline{K^*}$ [13]. We can not make a case that these shoulders are not an experimental distortion of the χ_2 line shape. However, a modest effort using Monte Carlo simulations has failed to produce a plausible explanation for them. We doubt that these enhancements are due to the $\eta_c(2S)$, since it would mean that the $\eta_c(2S)$ mass is well below its expected value and its decays to the $2(K^+K^-)$ and, especially, the $K^\pm K_s\pi^\mp$ final states are suppressed. These enhancements remain a mystery and require further investigation.

We have measured branching fractions for $\eta_c(1S)$ and $\chi_{c0,1,2}$ decays to $2(K^+K^-)$, $2(\pi^+\pi^-)$, $\pi^+\pi^-K^+K^-$, $\pi^+\pi^-p\overline{p}$, K_sK_s, $\phi\phi$, $\Lambda\overline{\Lambda}$, and $K^\pm K_s\pi^\mp$ final states. In a number of cases we see serious discrepancies with the PDG values for these decays.

In general, we find good agreement with results reported by C.Z. Yuan, with notable exceptions for for the $\pi^+\pi^-K^+K^-$ and $\phi\phi$ channels. The discrepancy in the former may be due to the different particle identification requirements that are used. For reasons we do not understand, we find that the event yields in this channel are especially sensitive to the details of particle identification criteria. The discrepancy in the $\phi\phi$ channel can be traced to a substantial difference in the value used for the acceptance.

5 Acknowledgements

This research is supported by the U.S. Department of Energy research grant number DE-FG03-94ER40833. This work was aided by my colleagues in the Hawaii BES group.

References

[1] C. Edwards *et al.* (Crystal Ball Collaboration), Phys. Rev. Lett. **48**, 70 (1982).

[2] W. Buchmüller and S-H.H. Tye, Phys. Rev. **D24**, 132 (1981).

[3] R.M. Barnett *et al.* (Particle Data Group), Phys. Rev. **D54**, 1 (1996).

[4] V. Vasilis and N. Byers, Phys. Rev. **D28**, 2908 (1983).

[5] K.T. Chao, Y.F. Gu, and S.F. Tuan *On Trigluonia in Charmonium Physics* University of Hawaii Preprint UH-511 790 94 (1993).

[6] Y.S. Zhu, *Recent ψ' and χ_c Results from BES*, invited talk at the XXCVIIIth International Conference on High Energy Physics, Warsaw, Poland, July 1996.

[7] J.Z. Bai *et al.* (BES Collaboration), *Branching fractions for ψ_{2S} decays to octet-baryon pairs*, paper submitted to the 1995 International Symposium on Lepton and Photon Interactions at High Energies, Beijing, China.

[8] X.H. Li and W.M. Dunwoodie, private communication.

[9] H. Albrecht *et al.* (ARGUS Collaboration), Phys. Lett. **B338**, 390 (1994).

[10] Chen Guang-Pei, private communication.

[11] S.L. Olsen, BES analysis memo: *Study of $\chi_c \rightarrow K^+K^-K^+K^-$*, November 1996, unpublished.

[12] C.Z. Yuan, talk at the January 1997 IHEP/BES monthly meeting; BES analysis memo: *Study of $\psi' \rightarrow \gamma$ + four charged tracks*, March 1997.

[13] S.L. Olsen, talk at the January 1997 US/BES meeting at Hawaii.

[14] W. Tannenbaum *et al.* (Mark I Collaboration), Phys. Rev. **D17**, 1731 (1978).

[15] R. Brandelik *et al.* (DASP Collaboration), Z. Phys. **C1**, 233 (1979).